Entry to the Stockholm Junior Water Prize 2009

Natural Organics Control Aggregation of Mercury Sulfide Nanoparticles in Freshwater Systems

Eileen Jang

United States of America

I. ABSTRACT

Mercury (Hg) is an environmental contaminant that is neurotoxic to humans, particularly to individuals exposed through consumption of fish. In aquatic environments, Hg-sulfides, such as HgS nanoparticles, are precursors to methylmercury, the form of Hg that bioaccumulates in fish. Current knowledge is limited regarding processes through which HgS nanoparticles persist. The goals of this study were to: 1) synthesize uncapped HgS nanoparticles, 2) characterize these nanoparticles, and 3) test aggregation rates of nanoparticles in solutions simulating natural conditions. A novel aqueous synthesis process for uncapped nanoparticles was developed using a controlled precipitation process. The resulting metacinnabar-HgS(s) was characterized through transmission electron microscopy, energy dispersive x-ray spectroscopy, and x-ray diffraction spectroscopy. Using dynamic light scattering, the aggregation rate of HgS nanoparticles was found to increase as salinity increased. Furthermore, the aggregation rate decreased in the presence of cysteine, an organic acid prevalent in sediment porewater. Through comparison of cysteine to a structurally-similar organic acid, serine, it is believed that the sulfhydryl group in cysteine is responsible for controlling aggregation rates. By studying the biogeochemical processes of these ubiquitous nanoparticles in aquatic systems, this research has deepened the understanding of mercury in its aqueous phase and furthered the emerging field of nanogeoscience.

II. TABLE OF CONTENTS

III. KEY WORDS

Mercury sulfide, nanoparticles, colloid aggregation, natural organic matter, nanogeoscience

IV. ABBREVIATIONS AND ACRONYMS

DLS: Dynamic Light Scattering

TEM: Transmission Electron Microscopy

EDS: Energy-dispersive X-ray Spectrocsopy

XRD: X-ray Diffraction

V. ACKNOWLEDGEMENTS

I would like to thank Dr. Helen Hsu-Kim of Duke University Pratt School of Engineering and her research group for allowing me to conduct research in the Hsu-Kim lab and for all of their guidance. I would also like to thank Dr. Myra Halpin and Mr. Robert Gotwals of the North Carolina School of Science and Mathematics for their assistance in this work. Appreciation is also extended to the Howard Hughes Precollege Program at Duke University. Lastly, I would like to thank my family for always supporting me and especially for supporting my research experience.

VI. BIOGRAPHY

I am currently a high school senior at the North Carolina School of Science and Mathematics in Durham, North Carolina. I have actively pursued an interest in the sciences by participating in science research, and leading the Science Olympiad and Health Occupations Students of America organizations at my school. I have taught an official school seminar for exploring medical careers and understanding the state of medicine in our world. I am also an active community volunteer, having volunteered at various community events and two community hospitals, and varsity softball player who has played softball since the age of four. I have presented my research in various settings, including the North Carolina Junior Science and Humanities Symposium, North Carolina State Science and Engineering Fair, Southeast Regional American Chemical Society Conference, and North Carolina International Science Challenge. Some of my high school accomplishments include National Merit Finalist, National AP Scholar, Siemens Competition in Math, Science & Technology Semifinalist, and Intel International Science and Engineering Fair Finalist.

1. INTRODUCTION

Mercury is a naturally-occurring element that can be found in all three phases in the environment. Specifically, in freshwater systems, the presence of mercury poses human health risks because mercury can be converted to methylmercury and bioaccumulate in the food supply. Most exposure to methylmercury comes from the consumption of seafood, freshwater fish, and shellfish; nearly all mercury found in fish is methylated [1]. Methylmercury has a strong affinity for sulfur-containing compounds such as proteins, making it a dangerous neurotoxin to humans and other mammals. Therefore, studying mercury sulfides allows one to understand the factors controlling the methylation process; that is, the amount of mercury sulfide present in a body of water also determines how much mercury will go through the the methylation process. The study of mercury sulfide and its geochemical properties is a fundamental starting point for understanding how mercury accumulates and travels in aqueous environments [2]. Figure 1 shows the pathway mercury can take as it makes its way into human bodies [3].

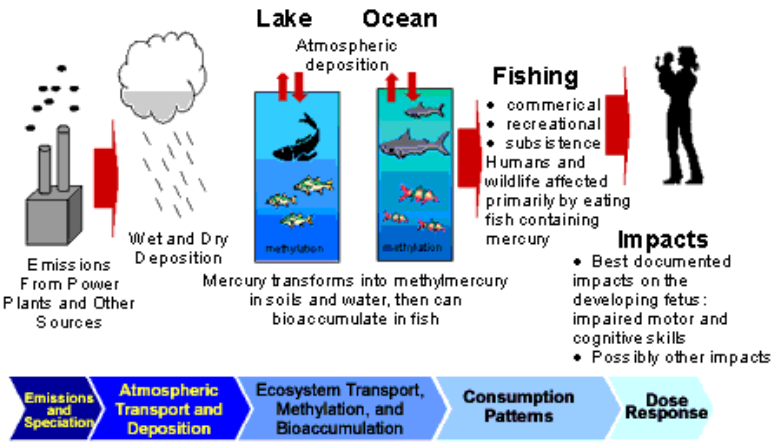

Figure 1*: Flowchart of how mercury enters the environment and impacts humans. [3]*

This study focuses on mercury sulfide on the nanoscale. Nanoparticles are a product of the nanophase that all minerals go through during formation, and are likely to persist when nucleation rates are high, and aggregated growth rates are slow. On the nanoscale, many minerals will behave much differently than they do on the macro or even microscopic crystal level [4]. In fact, previous studies have shown that the atomic structure of zinc-sulfide (sphalerite) nanoparticles differs from those of bulk zinc-sulfide [5]. In a natural environment, the stability of nanoparticle colloids can also be affected by natural organic matter, which is ubiquitous in all aquatic systems. Natural organic matter has been found to adsorb to iron oxide colloid surfaces to control aggregation and particle size [6]. In previous studies that attempted to include natural environmental conditions, humic acids and thiol-containing organic acids were shown to stabilize the growth rate of zinc-sulfide nanoparticles in aqueous environments. The mechanism thought to be responsible for the stabilization is the adsorption of the organic acids to the surface of nanoparticles [7].

The objectives of this study were to synthesize mercury sulfide nanoparticles, characterize these nanoparticles, and study the rate of aggregation of these nanoparticles with respect to ionic strength and natural organic acids in the environment. Ionic strength was controlled in order to model salinity in natural waters, while natural organic acids were used to model natural organic matter. The results indicated that ionic strength plays an important factor in aggregation rates and organic acids are effective in controlling particle growth. Furthermore, by testing two organic acids that are identical in structure with the exception of a hydroxyl functional group in the place of a sulfhydryl functional group, it was found that the sulfhydryl group is essential in influencing aggregation rates.

2. EXPERIMENTAL SECTION

Materials

All chemicals utilized for this research were ACS reagent grade from Fisher Scientific, unless otherwise noted. Ultrapure water (Barnstead Nanopure, >17.8 MΩ-cm) was used to prepare all stock solutions. Trace-metal grade acids were used for pH adjustments. Ultra high purity nitrogen (N_2) was used as needed for purging steps. All glass containers and any fluoropolymer-lined caps were acid-cleaned through soaking overnight in 1 M HCl, followed by a three-times rinse with ultrapure water. Hg stock solutions consisted of $Hg(NO_3)_2$ dissolved in 0.1 M HNO_3. Sulfide stock solutions were prepared by dissolving crystals of $Na_2S{\cdot}9H_2O$ (rinsed with ultrapure water and dried prior to weighing) in N_2-purged ultrapure water. Sulfide and cysteine stock solutions were stored at 4°C and utilized within 24 hours of preparation. Serine stock solutions were also stored at 4°C and utilized within one week of preparation.

Synthesis and characterization of nanoparticles

Nanoparticles were defined as particles between 1 to 100 nm in hydrodynamic diameter. This study attempted to synthesize mercury sulfide nanoparticles using two approaches. The first method of mixing equal molar concentrations of mercury and sulfide produced unstable nanoparticles that grew in size over time (minutes). The second approach of preparing a base solution in ultrapure water of mercury nitrate and injecting sodium sulfide produced stable nanoparticles of varying sizes. In rapid succession, sodium hydroxide, NaOH, and sodium sulfide, Na_2S, were injected into the mercury nitrate solution. The sodium hydroxide was used to control the pH of the solution. The mercury sulfide suspension was stirred using a stirring plate and stir bar for at least ten minutes. The nanoparticles were left untouched overnight to allow for stabilization. All test samples were prepared under ambient laboratory (i.e., oxic) conditions. Transmission electron microscopy (TEM), energy dispersive x-ray spectroscopy (EDS), and x-ray diffraction (XRD) were then used to characterize and confirm mercury sulfide samples.

Aggregation kinetics of nanoparticles

Experiments were done in 4 mM sodium 4-(2-hydroxyethyl)piperazine-1-ethanesulfonate (HEPES) buffer at pH 7.50, and various concentrations of $NaNO_3$ between 75 mM and 1 M that controlled the ionic strength. The buffer solutions were filtered using 0.2 µm nylon syringe filters (VWR International) to ensure no dust or other particles were present that may have increased extra surface area for nanoparticles to aggregate on and therefore increased error in aggregation rate. Buffer solutions were stored in glass bottles that had been acid washed and air dried in a laminar flow hood.

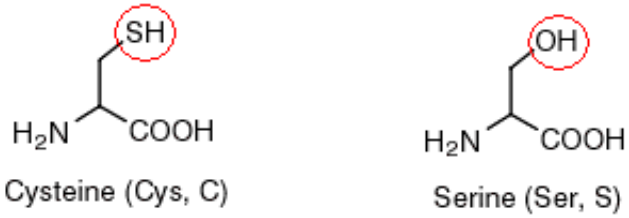

Figure 2: *Structure of the organic acids serine and cysteine, which differ only in a sulfhydryl functional group.*

Cysteine and serine were the primary organic acids studied. Cysteine and serine are low-molecular weight organic acids that were used because they have well-defined structures. As shown in Figure 2 above, serine has a structure identical to that of cysteine with the exception of a hydroxyl group (-OH) in place of the sulfhydryl group (-SH). Therefore, the comparison of aggregation rates between adding cysteine and serine allowed for determining whether a specific functional group was responsible for the changes in aggregation rate of nanoparticles.

Samples were prepared by adding a buffer solution of the intended ionic strength to a polypropylene or glass vial. For experiments containing an organic acid, organic acid was added to the buffer solution. A 1:100 dilution of mercury sulfide particles to buffer solution was then injected into the solution. An aliquot was taken from the matrix to be tested using dynamic light scattering (DLS), which monitored nanoparticle aggregation rates. DLS theory is well-established and often used to measure growth rates of small particles in the nanometer to micron range over time. For monitoring aggregation rates in different ionic strengths and in the presence of organic acids, the average hydrodynamic diameter was estimated every 7 minutes by averaging 15 to 24 individual 10-second measurements. In the case of aggregation rates where a significant amount of growth occurred within 7 minutes, a shorter time period with a lower number of individual measurements was used in order to capture the fast growth rate. The

average hydrodynamic diameter was then estimated every 2 minutes by averaging 13 individual 10-second measurements. Aggregation rates were found by taking the slope of the linear portion of the aggregation curve, which leveled off with time. The time range over which the linear portion lasted for aggregation was determined based on the rate of aggregation. Taking the slope of the linear portion of individual graphs allowed for accurate comparison of aggregation rates. Linear portions had acceptable R^2 values that were greater than 0.9.

3. RESULTS AND DISCUSSION

Characterization of products of synthesis

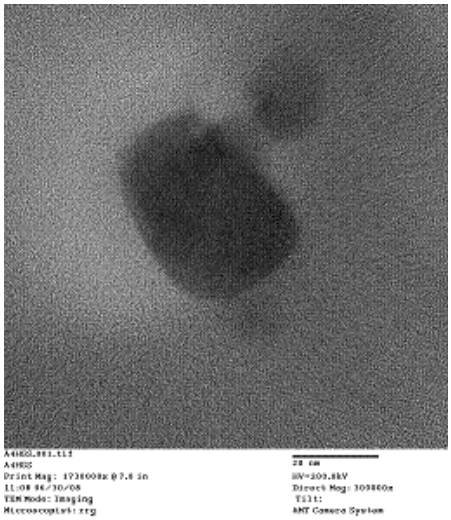

Figure 3: *TEM image of nanoparticles. Scale bar = 20 nm, horizontal line located on lower right corner.*

TEM imaging was first used to confirm the presence of mercury sulfide nanoparticles after the synthesis process. In Figure 3, an image of a single nanoparticle in solution is shown. The solution of nanoparticles was not completely homogeneous, but differences in sizes were expected due to an uncapped synthesis process where ligands could not be used to easily control particle size. During dynamic light scattering, hydrodynamic diameter was measured as an average, which accounted for any difference in sizes of particles in solution.

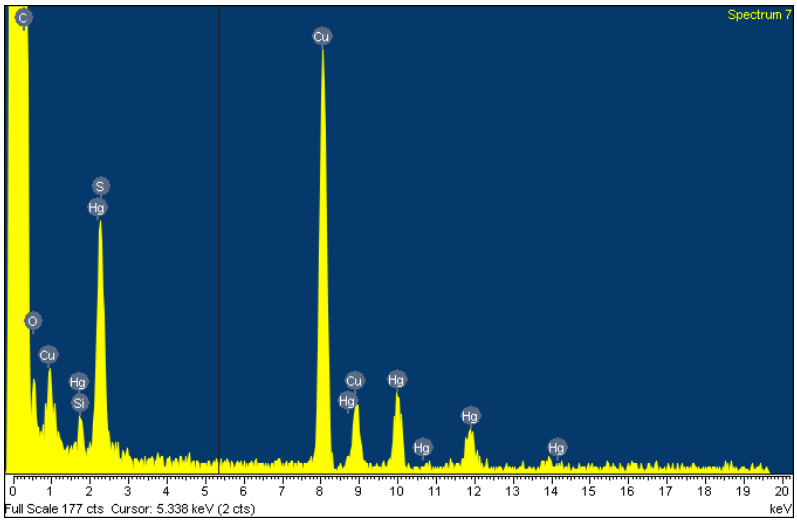

Figure 4: *EDS spectra for mercury sulfide nanoparticles.*

EDS, shown in Figure 4, was used to confirm that the elements mercury and sulfur were indeed in the sample. EDS also showed that carbon, copper, silicon, and oxygen were present in the sample, but these elements were accounted for by the sample holder used for EDS.

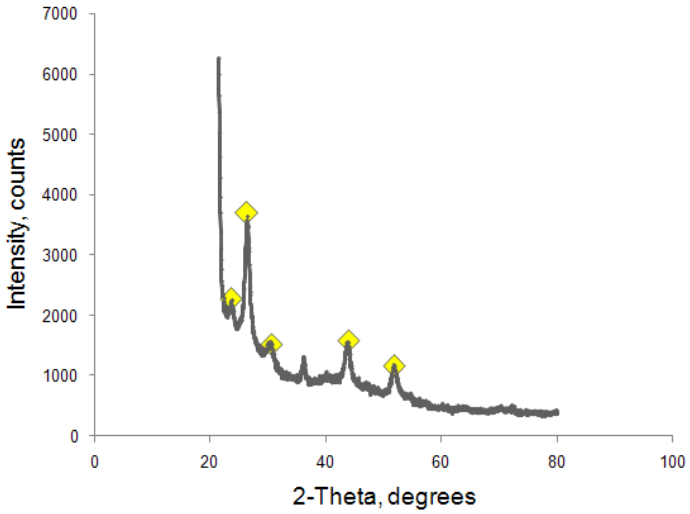

2-Theta (degrees)	**Intensity** (counts)
23.62	2271
26.34	3693
30.58	1530
43.86	1591
51.82	1160

Figure 5: *The XRD diffraction pattern for mercury sulfide nanoparticles is shown on the left. The emphasized points denote the peaks that match known metacinnabar XRD peaks [8]. These points, shown in the table on the right, are at: 23.62, 26.34, 30.58, 43.86, and 51.82 degrees. Other peaks in the image are due to the background membrane material, and thus are not considered peaks that serve to identify metacinnabar mercury sulfide in the sample.*

In order to characterize the sample as either cinnabar or metacinnabar mercury sulfide, the two most commonly found forms of mercury sulfide in nature, XRD, were utilized. The XRD diffraction pattern

can be seen in Figure 5. The peak positions on the XRD spectra, which are emphasized with diamond-shaped points, corresponded with values found in previous literature and international databases [8] for metacinnabar mercury sulfide, also known as β -HgS.

Thus, based on the various methods of characterization discussed in this section, the synthesis process used to form mercury sulfide nanoparticles was shown to form metacinnabar mercury sulfide nanoparticles between 1 to 100 nm in size.

Effects of salinity on aggregation

Once mercury sulfide nanoparticles were synthesized, they were put into solutions of varying ionic strength in order to study the effect of salinity on nanoparticle aggregation rates. Aggregation rates were estimated as a function of ionic strength using a $NaNO_3$ background electrolyte. Ionic strength was determined solely through the concentration of the $NaNO_3$ through the following equation:

$$I = \frac{1}{2}\sum_{B=1}^{n} c_B z_B{}^2$$

where c_B is molar concentration of ion B and z_B is the charge number of ion B.

The aggregation rate over time is represented as $\frac{dD_H}{dt}_{t\to 0}$.

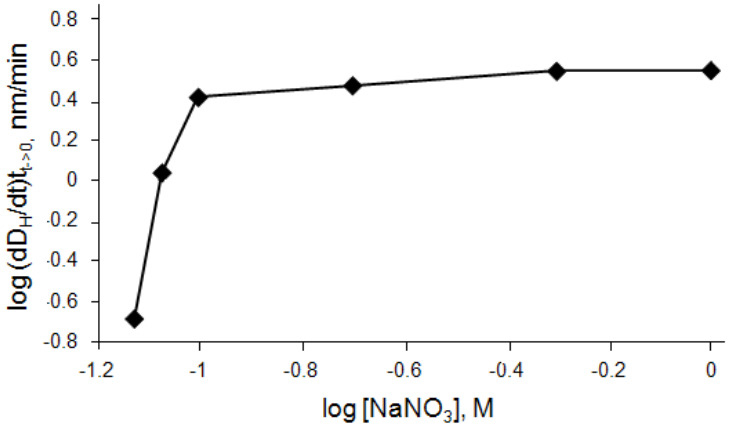

Figure 6: *A logarithmic graph of* $\frac{dD_H}{dt}_{t\to 0}$ *(nm/min) versus concentration of* $NaNO_3$ *(M). An initial increase in* $\frac{dD_H}{dt}_{t\to 0}$ *is seen before the rate levels off, signaling that the increase in concentration of* $NaNO_3$ *no longer increases aggregation rate.*

In terms of ionic strength, as the concentration of $NaNO_3$ increased, $\frac{dD_H}{dt}_{t\to 0}$ increased until it leveled off at around a $NaNO_3$ concentration of 200 mM. A likely mechanism for explaining this pattern is as follows: as $NaNO_3$ concentration was increased in a solution, the thickness of the diffuse ion layer surrounding the particles was suppressed, leading to more successful collisions, thus increasing $\frac{dD_H}{dt}_{t\to 0}$. However, at 200 mM, the change in $NaNO_3$ concentration was no longer effective in increasing the magnitude of the charge of nanoparticles, indicating that Brownian motion was the only limit to controlling aggregation. In natural waters, this would lead one to believe that the salinity of surrounding waters can only control the aggregation rate of mercury sulfide nanoparticles up to a certain point. In this case, at that point in the graph in Figure 6, it can be seen that $\frac{dD_H}{dt}_{t\to 0}$ remains constant. This maximum value is designated as the diffusion-limited growth rate $\frac{dD_H}{dt}_{fast;\, t\to 0}$.

Effects of organic acids on aggregation

In order to determine the effects of organic acids on nanoparticle aggregation, a set of equations was used:

The aggregation rate of nanoparticles was found by measuring the increase in hydrodynamic diameter, D_H, over time:

$$\frac{dD_H}{dt} \propto kn_0$$

The product of the aggregation rate constant, k, and the colloid concentration, n_0, is proportional to the slope of the linear portion of the aggregation curve over time. Furthermore, a ratio of the measured aggregation rate constant, k, to the diffusion-limited (fast) aggregation rate constant k_{fast} can be calculated using the following equation:

$$\frac{dD_{H_{t\to 0}}}{dD_{H_{fast;t\to 0}}} = \frac{k}{k_{fast}}$$

The ratio of the aggregation rate constant to the diffusion-limited aggregation rate constant can also be written as:

$$\frac{1}{W} = \alpha$$

The inverse stability ratio is represented by $\frac{1}{W}$, and is also equivalent to α, or the attachment efficiency, which is the fraction of collisions that resulted in attachment.

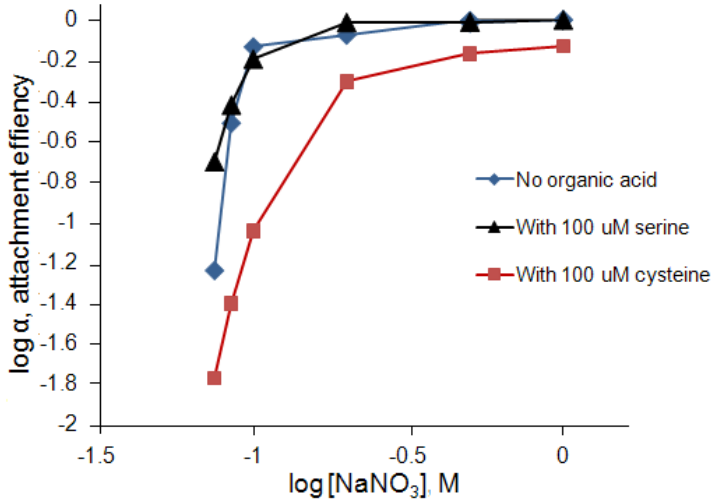

Figure 7: *A logarithmic graph of the attachment efficiency, α, versus concentration of $NaNO_3$ (M). The blue data points (marked with diamond-shaped points) indicate α of nanoparticles in a buffer solution with no organic acid. The black data points (marked with triangle-shaped points) indicate α of nanoparticles in a buffer solution with 100 µM serine added. The red data points (marked with square-shaped points) indicate α of nanoparticles in a buffer solution with 100 µM cysteine added.*

Cysteine was found to act as an organic surfactant, or capping agent, that stabilized the growth of nanoparticles. In the presence of cysteine, the attachment efficiency, α, was found to be less in solutions of any ionic strength of those investigated. Serine, however, showed no effect in changing α in solutions of any ionic strength. Attachment efficiency values were close to those of the particles in a solution with no organic acid. This leads one to believe that the sulfhydryl functional group is responsible for stabilizing the nanoparticles in solution and reducing the fraction of collisions that resulted in attachment, as the only difference in cysteine and serine is that the sulfhydryl functional group found in cysteine is replaced by a hydroxyl functional group in serine. Figure 7 displays the attachment efficiency of nanoparticles in a buffer solution alone, in a solution with 100 µM cysteine, and in a solution with 100 µM serine. The attachment efficiency values seen for nanoparticles in a buffer solution alone and in a solution with 100 µM serine follow each other very closely, while the

attachment efficiency values seen in nanoparticles in a solution 100 µM cysteine are stunted and below the attachment efficiency values for the other two solutions.

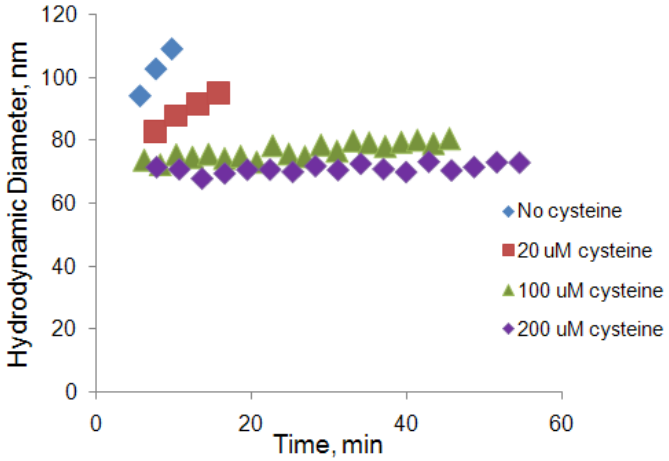

Figure 8: *A graph of hydrodynamic diameter (nm/min) versus time (min). The different trends on the graph represent the aggregation rates of nanoparticles of solutions of different cysteine concentrations from no cysteine to 200 µM cysteine. As the cysteine concentration increased, the aggregation rate decreased.*

As the concentration of cysteine is increased, aggregation rate is further decreased. This can be explained because as the concentration of cysteine is increased, more cysteine adsorbs to the surface of the nanoparticles. As the surfaces of the nanoparticles are modified by adsorbed cysteine, the frequency of successful collisions between particles decreases. Therefore, there is a decrease in the aggregation rate $\frac{dD_H}{dt}$. The effects of increasing concentrations of cysteine on growth of aggregates can be seen in Figure 8.

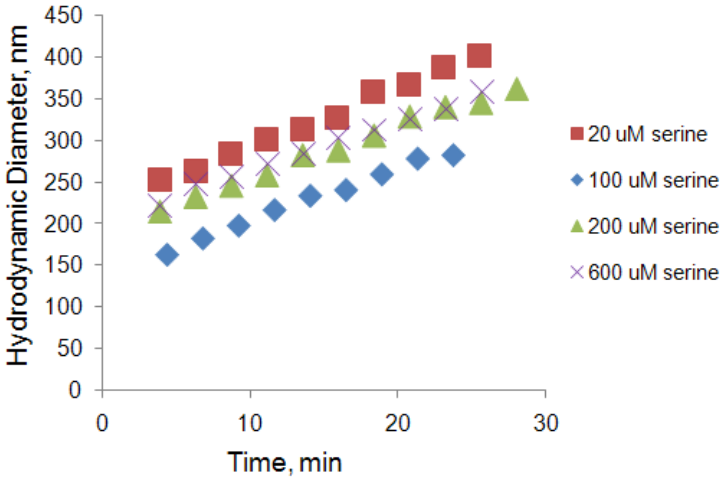

Figure 9: *A graph of hydrodynamic diameter (nm/min) versus time (min). The different trends on the graph represent the aggregation rates of nanoparticles of solutions of different serine concentrations from no serine to 600 µM serine. As the serine concentration increased, the aggregation rate stayed constant.*

As the serine concentration increased to the same levels as the cysteine concentration, there were no significant decreases in aggregation rate, as shown in Figure 9. This falls in line with Figure 7, which demonstrated that serine did not change aggregation rate, or change in size over time, in solutions of differing ionic strength while cysteine did. Therefore, cysteine produces an aggregation curve with lower values of $\frac{dD_H}{dt}$ in solutions of different ionic strength, and also decreases aggregation rate as its concentration is increased. Serine produces a curve with the same values of $\frac{dD_H}{dt}$ (no significant differences in $\frac{dD_H}{dt}$ values) as the aggregation curve with bare particles colliding in buffer solutions of varying ionic strength, and does not decrease aggregation as its concentration is increased.

These experiments have shown that indeed, salinity and natural organic acids do play a role in controlling the aggregation of nanoparticles. These results agree with previous literature, which showed that natural organic matter played a role in controlling the aggregation of iron oxide nanoparticles [4]. This study can be used as a starting point for studying the mechanism through which the sulfhydryl functional group stunts aggregation of nanoparticles and affects their surface chemistries.

In a wider scientific context, understanding natural and synthetic nanoparticle processes and their overall impact on earth systems is the challenge for the future. Very little is known about the environmental implications of nanoparticle chemistry. The consequences of developing nanotechnologies in various fields are unknown because nanoparticles have been treated as if they were part of their crystalline and microscopic counterparts, and the actual mass distribution of nanomaterials and mineral nanoparticles is unknown [4]. Tying into the consequences of developing nanotechnologies is the field of nanotoxicology. Nanotoxicology investigates the effects of nanostructures on the human body. Potential bioaccumulation and dangerous pathways for synthesized nanomaterials to be carried into both humans or natural ecosystems need to be studied. This study was a step forward in understanding mercury sulfide nanoparticles processes and behaviors in freshwater systems.

Specifically in the case of mercury sulfide, because mercury sulfide nanoparticles can be found between 1 to 100 nanometers in size, they are able to pass through conventional filters and may be

misclassified as soluble, thus affecting predicted mercury levels. By identifying the conditions that allow mercury sulfide nanoparticles to aggregate and stabilize on a watershed level, this research will facilitate modeling water quality levels in anaerobic sediments and other waters such as those of municipal wastewater treatment plants and estuaries near large urban centers.

4. CONCLUSION AND FUTURE WORK

This study has successfully: 1) used a novel synthesis process to produce mercury sulfide nanoparticles under 100 nm in size, 2) characterized these nanoparticles as metacinnabar, or β-HgS, and 3) tested the aggregation rates of HgS nanoparticles in solutions simulating natural freshwater conditions. A novel synthesis process producing mercury sulfide was developed using a controlled precipitation process and used a base solution of mercury nitrate with injections of sodium sulfide. The synthesized nanoparticles were characterized as metacinnabar-HgS(s) between 1 to 100 nm in diameter through transmission electron microscopy, energy dispersive x-ray spectroscopy, and x-ray diffraction spectroscopy. Nanoparticles were found to aggregate faster in solutions of higher ionic strength until around 200 mM $NaNO_3$, at which point the aggregation rate was likely limited by Brownian motion. Aggregation rates were also tested in the presence of the organic acids cysteine and serine, which are structured similarly with the exception of one functional group. Aggregation rates were lowered at all ionic strengths when cysteine was present in a solution, but remained the same when serine was present in a solution. Also, aggregation rates were found to further decrease as cysteine concentration increased, but aggregation rates showed no significant differences as serine concentration increased. Therefore, the sulfhydryl functional group, which is found only in cysteine, is thought to be responsible for the reduction in aggregation rate.

This study suggests that cysteine acts as an organic surfactant that adsorbs to the surface of mercury sulfide nanoparticles to stunt aggregation of particles. In terms of future work, the next step is to confirm that adsorption of cysteine is occurring on the nanoparticles by quantifying the partitioning of cysteine between particles and water.

Another point of interest for future work is modeling and quantifying the interactions between mercury sulfide and natural organic matter through computational research. Using various computing methods, the interactions of mercury sulfide and natural organic matter can be closely observed in a controlled system.

On a broader scale, the bioavailability of mercury held in the form of mercury sulfide nanoparticles is an important factor in deciding whether or not mercury is available to be methylated. Two main focuses of future work will be studying how methylation rates are influenced by mercury sulfide nanoparticle processes and how mercury sulfide nanoparticles influence bioavailability of mercury in the environment, both of which are important to understand in preventing methylmercury poisoning in humans and other organisms.

5. REFERENCES

[1] Bloom, N.S; Watras, C.J.; Hurley, J.P. Impact of Acidification of the methylmercury cycle of remote seepage lakes. *Water Air Soil Pollu*. 1991, 56, 477-491.

[2] Ravichandran, M. Interactions between mercury and dissolved organic matter-a review. *Chemosphere* 2004, 55, 319.

[3] "Human Exposure to Mercury." 29 August 2008. United States Environmental Protection Agency. 21 September 2008. <http://www.epa.gov/mercury/exposure.htm>.

[4] Hochella, Michael F. Jr; Lower, Steven K.; Maurice, Patricia A.; Penn, R. Lee; Sahai, Nita; Sparks, Donald L.; Twining, Benjamin S. Nanominerals, Mineral Nanoparticles, and Earth Systems. *Science* 2008, 1631, 319.

[5] Gilbert, B.; Banfield, J. F. Molecular-scale processes involving nanoparticulate minerals in biogeochemical systems. *Rev. Miner. Geochem.* 2005, 59, 109-155.

[6] Mylon S.E.; Chen K.L.; Elimelech M. Influence of natural organic matter and ionic composition on the kinetics and structure of hematite colloid aggregation: Implications to iron depletion in estuaries. *Langmuir* 2004, 20, 9000-9006.

[7] Lau, B.; Hsu-Kim, H. Precipitation and growth of Zn-sulfide nanoparticles in the presence of thiol-containing natural organic ligands. *Environ. Sci. Technol.* 2008, in press.

[8] Downs, R.T. and Hall-Wallace, M. The American Mineralogist Crystal Structure Database. *American Mineralogist* 2003, 88, 247-250.